Does Collarette of Iris Work for Recognizing Persons?

Ren-He Jeng, Wen-Shiung Chen
VIP-CCLab., Dept. of Electrical Engineering
National Chi Nan University
Puli, Nantou, Taiwan
s98323907@mail1.ncnu.edu.tw, wschen@ncnu.edu.tw

Lili Hsieh
Dept. of Information management
Hsiuping University of Science and Technology
Taichung, Taiwan
lily@mail.hust.edu.tw

Abstract—In recent years, iris has been extensively discussed in the field of biometrics. An iris recognition system has three main stages such as image preprocessing, feature extraction and template matching. Since eyelid and eyelashes act as a kind of armour that protect the eye from harm, it makes iris localization inaccurate in image pre-processing step. A novel method is proposed to locate iris radius based on collarette of iris muscle. The collarette is the thickest region of the iris, separating the pupillary portion from the ciliary portion. Some researches suggest that the parameters of iris normalization algorithm adopts collarette to replace iris outer radius. However, reducing the normalization radius of iris will deform normalized iris image and result in lose of iris feature information. In this paper, we present our experiments by adopting different iris radii and different normalization algorithms in iris recognition system. We also propose an iris localization method and a collarette localization method. In feature extraction, we adopt the Gabor wavelet filter to extract local texture features from iris images. All experiments are tested on UBIRIS Sessao.1 and CASIA.v1 databases. The experimental results show that the proposed approach has achieved a high accuracy of 96%.

Keywords-Biometrics; Iris Recognition; Iris Localization; Iris Normalization; Collarette;

I. INTRODUCTION

In biometric-based automatic identity authentication techniques, iris recognition is one of the most reliable and trusted methods. Human iris is a thin circular organ which lies between the cornea and the sclera of a human eye. Literature show that, among all the biometric traits, iris has most rich texture information and very high uniqueness, which has been proved in the first automated iris recognition system developed by Daugman in [1]. In his system, a human iris is localized by using the integro-differential operators and then the cropped iris region is linearly normalized to rectangular image. Following the preprocessing step, 2D Gabor wavelets are used to extract iris codes based on the sign of the phase angle, and the iris codes are matched by using Hamming distance.

Another well-known iris recognition system was proposed by Wildes et al. [2], in which the Hough transform is applied to locate iris and the Laplacian pyramid is used to extract four band-pass components from one iris image as their feature presentation. Typically, the framework of iris recog-

nition systems includes three steps: image preprocessing, feature extraction, and classification/recognition. In fact, the key step is to detect the range of interesting in the image preprocessing part. This key step is sometimes called the normalization step and it effects the system recognition performance drastically. The general normalization algorithm was proposed by Daugman [1]. This algorithm is the most popular and has been widely used in many systems, in which irises are assumed in a homogenous "rubber-sheet" model. In Daugman's approach, the annular iris region is linearly mapped or transformed into a fix-sized rectangular block via the following formulas:

$$\begin{cases} x\left(r, \theta\right) = \left(1 - r\right) x_p\left(\theta\right) + r x_i\left(\theta\right) \\ y\left(r, \theta\right) = \left(1 - r\right) y_p\left(\theta\right) + r y_i\left(\theta\right) \end{cases} \quad (1)$$

where $(x_p(\theta), y_p(\theta))$ and $(x_i(\theta), y_i(\theta))$ are the polar coordinates of the inner and outer boundary points in the direction θ in the original image, (x, y) are the Cartesian coordinates. In 2000, H. J. Wyatt's [3] proposed a mesh-work of 'skeleton' that can minimize 'wear-and-tear' of iris as pupil size varies. By following, Yuan and Shi [4] adopted the idea in [3] as a basic model and simplified it, and developed a non-linear iris normalization model algorithm. The modified approach was applied to overcome the non-linear deformation on the iris texture caused by pupil variations. It has been shown that this modified approach achieves a relatively good performance. However, the model needs to solve two simultaneous equations, it is complicated to get the sampling points and the time complexity is high. Moreover, the model is not entirely accurate since it assumes the stretch of iris tissue in radial direction is linear as the pupil size changes. Changing the size of pupil is controlled by iris with sphincter muscle and radial muscle from different expanded level of direction. Therefore, to develop a non-linear normalization method for resolving iris texture deformation is necessary.

Though the eyelid and eyelash protect the iris of a human eye, the blocking from them actually affects the processing of image preprocessing step such that almost all systems are not capable of precisely locating the radius of an iris. Accordingly, some research works focus on how to locate the iris precisely. One of the works is to localize the so-called

"collarette" [5] [6], which is a clear division line between sphincter muscle and radial muscle, as illustrated in Fig. 1. Some researchers believe that the colleratte may replace iris outer radius potentially and improve the performance of iris recognition systems. In 2004, Sung *et al.* [5] proposed a framework of iris recognition with collarette detection algorithm for locating boundary using statistical information, and the success rate increases 1.0%. This system was tested in two fields, one is between inner boundary and outer boundary and another is between inner boundary and collarette boundary.
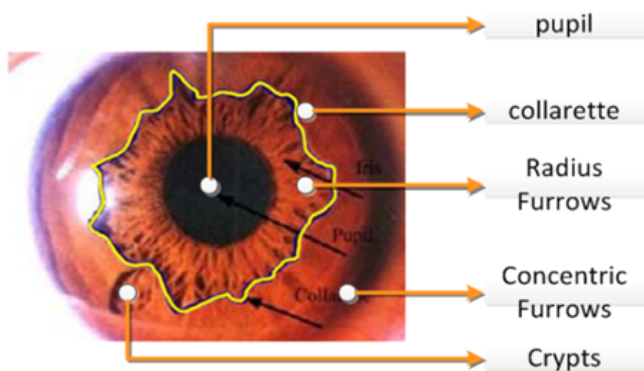

Figure 1.   The structure of a human iris.

II. OUR METHOD

A. Iris Localization

The framework of our recognition system is shown in Fig. 2. In the image preprocessing part, there are three processes such as initial iris localization, collarette detection, and normalization. Our proposed collarette detection method has a limited condition for initial iris localization radius due to collarette zone, which is the region between iris outer radius and iris inner radius. Accordingly, the initial iris radius could wrap collarette. If initial iris radius could not provide enough normalization radius, it does not illustrate collarette in unwrapping image.
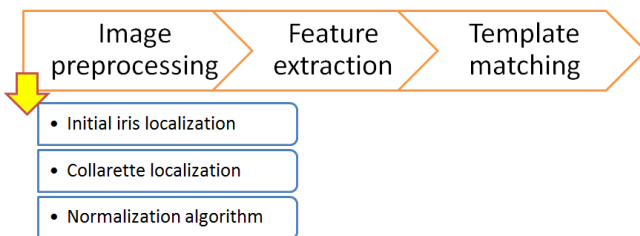

Figure 2.   The framework of the iris recognition.

1) Initial Radius Localization: Initial radius localization consists of four operations in the following: segmentation, *k*-means computation, boundary points detection and radius localization, as shown in Fig. 3. First, we must assume a center point, radius and segmentation range for segmenting assumed iris zone, as shown in Fig. 4 (a)(c). Besides, we used pixel intensity of slices to decide initial boundary, as $S_i = \max |\mathrm{P}_i - u_i|$, where S_i is boundary, P_i is pixel intensity, and u_i is the mean value of each slice. A slice means a serial of pixels. Then the initial radius initial is defined to be the mean value of S_i. Following, in the second part, we used *k*-means algorithm to cluster color features, as illustrated in Fig. 4 (b)(d). Moreover, we find the closest different value with value on index initial of slice, which are radius points r_p, as illustrated in Fig. 4 (e). Finally, the r_p points are mapped onto original eye image, and then the mean values of axis-x and axis-y are the coordinates of the initial radius center point, due to the instinctive symmetry in the shape of irises. In fact, the radius is the mean of distances between center points and r_p.

Figure 3.   The flow diagram of initial radius localization.

2) Collarette Localization: In the beginning, we refer to "pushing and pulling" model [7] to develop our proposed initial radius localization. After unwrapping iris by eq. 1 with initial radius, we observe pixel intensity of the slices, as shown in Fig. 5(a), it is an example curve about pixel intensity in three angles. Since the trend of curves are upwards, our goal is to find the points where the intensity changes from flat into upwards in every curves. Figure 5(a) that the curves are not smooth so that it might be located at local parts. Accordingly, we construct a curve in polynomial curve fitting [8], as illustrated in Fig. 5(b), that has the best fit to a series of data points, possibly subject to constraints.

When computing the mean value u_i in *i*-th curve (L_i), we find the closest point in the curves $P_i = \min |L_i - u_i|$, as illustrated in Fig. 6, and the real-line is the simulated collarette line. And then computing the mean of P_i, we obtain the position index of the collarette in iris unwrapping image. Finally, by re-mapping the pseudo collarette to original iris, the real collarette radius is then detected.

B. Iris Normalization

Since the location of the iris is known, our experiments are tested on UBIRIS.v1 series 1 and CASIA.v1 with linear normalization and non-linear normalization algorithm, respectively. The linear normalization was proposed by Daugman [1], and in this paper we will introduce a non-linear normalization algorithm in the following subsection.
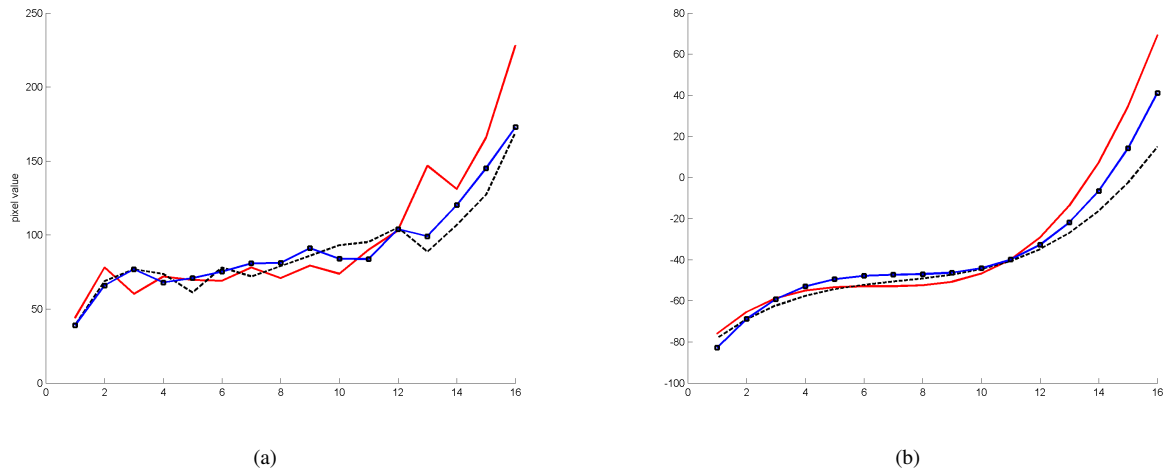
Figure 5.   The pixel value samples of an iris.

1) Fast Algorithm of Non-Linear Normalization: According to the method in the non-linear normalization model [3], [4] mentioned above, we know that the final goal is to find out the Cartesian coordinates A_x and A_y of the sampled point A, indirectly by first knowing the coordinates of the virtual point A'. If we know the length of $\overline{OA}$ between the point A and the pupil center O, and the angle $\theta_r(i)$ between $\overline{OA'}$ and y-axis, the coordinates of the point A may be determined. It is observed from Fig. 7 that the two points A' and A are collinear, so $\overline{OA}$ and $\overline{OA'}$ have the same angle $\theta_r(i)$. Obviously, the three points, the point A', the pupil center O and the center o_1 of $arc(P'I')$, form a triangle $\triangle A'Oo_1$, as shown in Fig. 7. Since the lengths of three sides of the triangle are known, the angle $\theta_r(i)$ can be determined according to the law of cosine.

Similarly, the three points, the point A, the pupil center O and the center o_2 of $arc(PI')$, also from another triangle $\triangle AOo_2$, as shown in Fig. 7. In this triangle only $\overline{OA}$ is unknown. According to the law of cosine, the length of $\overline{OA}$ may be determined from $\theta_r(i)$ which might be obtained from $\triangle A'Oo_1$. Trivially, the coordinates, A_x and A_y, of the sampled point A are computed by the following equations:

$$\begin{cases} A_x = \Delta_1(i)\sin(\theta_r(i)) \\ A_y = \Delta_1(i)\cos(\theta_r(i)) \end{cases} \quad (2)$$

where

$$\theta_r(i) = \cos^{-1}\left[\frac{y_2^2 + (r_{ref} + \Delta_2(i))^2 - r_2^2}{2y_2(r_{ref} + \Delta_2(i))} \right] \quad (3)$$

and

$$\Delta_1(i) = \left(r_1^2 + y_1^2 - 2y_1 r_1 \cos(\theta_k(i)) \right)^{1/2} \quad (4)$$

with

$$\theta_k(i) = \sin\left(\pi - \sin(\theta_r(i)) - \frac{y_1\sin(\theta_r(i))}{r_1} \right) \quad (5)$$

Finally, we adopt the cartesian coordinates of all of the sampled point A on $arc(PI')$ to construct a non-linear normalization model directly. The detailed procedure is shown in algorithm

---
Algorithm 1 Fast Non-Linear Normalization Algorithm

1: **FOR** $i = 1$ to $m - 1$ **do**
2:     Compute $\theta_k(i)$;
3:     Compute $\Delta_1(i)$;
4:     Compute $\theta_r(i)$;
5:     $A_x = \Delta_1(i)\sin(\theta_r(i))$;
6:     $A_y = \Delta_1(i)\cos(\theta_r(i))$;
7: **END**

C. Iris Enhancement

First, we use linear normalization and non-linear normalization to transform the detected iris region into 128×32 and 64×64 rectangular iris image, respectively. Then the mean of pixel is computed for each block of size 16×16, and these means are processed by bi-cubic interpolation to estimate the background illumination. After the background illumination factor is reduced, the local histogram equalization is conducted to reveal the details of the iris texture.

D. Feature Extraction

Feature extraction is used to reduce the data size of the image and to extract the key features. Therefore, we adopt 2D Gabor wavelets [1] to extract features. We only store a small number of bits for each iris code, so the real and imaginary parts are each quantized. To perform this task, we
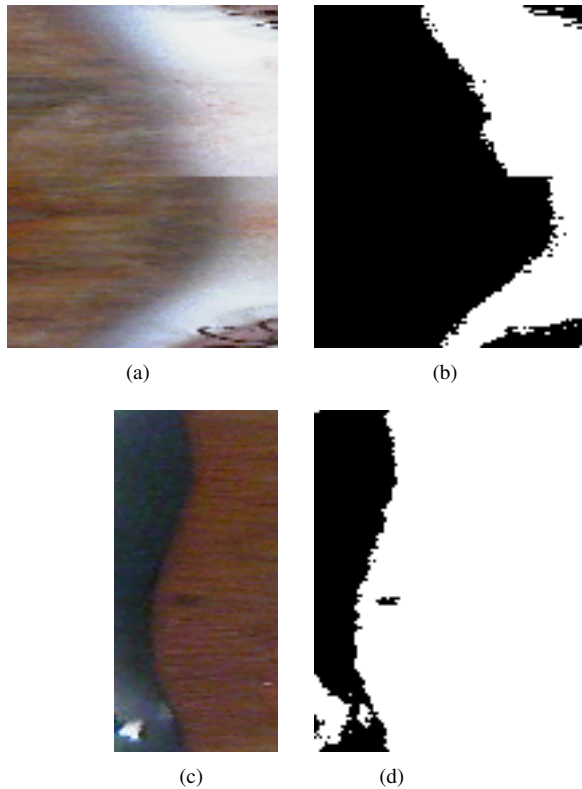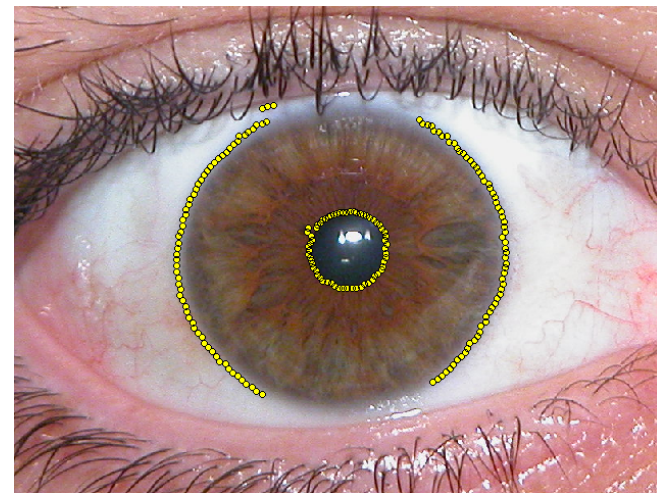
(a)   (b)

(c)   (d)

(e)

Figure 4.   The example result of radius localization.
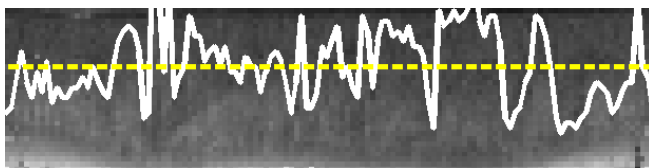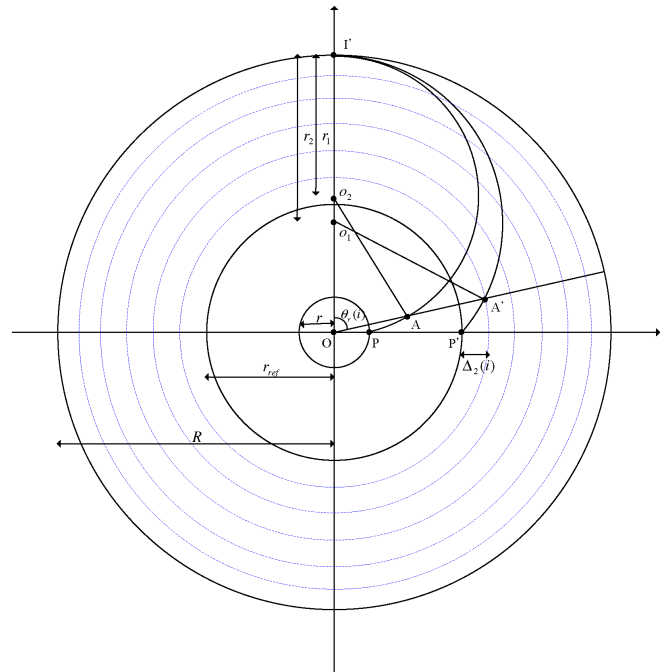

Figure 6.   The simulated collarette line.

Figure 7.   Fast non-linear normalization model.

measure the Hamming distance [1] between two iris codes and then set threshold to recognize them.

III. EXPERIMENTS AND ANALYSIS

A. Iris Database Description

Our experiments for identification will be tested on UBIRIS.v1 Sessao 1 and CASIA.v1 database, respectively. The UBIRIS.v1 Sessao 1 [9] has 241 people for a total 1214 images and at least 5 photos in each class of size 800×600, and taken at a moderate distance under visible wavelength light and the primary objective is to reduce the need for cooperation, which means the users would not feel constrained during the process of image acquisition. It is developed by the SOCIA lab (Soft Computing and Image Analysis Group) of the University of Beira Interior. In the CASIA.v1 database [10], there are 756 images for 108 people and least 7 photos in each class of size 320×280, and captured by near infra-red camera automatically in room.

B. Comparison of the Sampling Distances with Different Iris Radius Sets

In this paper, we tested iris recognition system with different normalization algorithms, linear normalization algorithm and non-normalization algorithm, and different radius. For the unwrapping part, we tested three fields. The first field is between inner boundary and outer boundary, the second one is between collarette and outer boundary, and the third one is the field between inner boundary and collarette boundary.

As iris radius and collarette were detected, we computed the difference value between the coordinates of *i*-th and (*i*+1)-th sample points, as shown in Fig. 8. Since the image size of eye in CASIA is smaller than UBIRIS.v1 Sessao 1, the sampling distance curves are beating lightly in Fig. 8 (c)(d).

C. Experimental Results

In our experiments, we define three iris radii: iris inner (*ir*), iris outer (*IR*) and collarette (*cr*). In fact, all experiments are tested in three wrapping fields with *ir-IR*, *ir-cr* and *cr-IR*. As mentioned in previous section, we extract iris features by using 2D-Gabor wavelet filter, store a small number of bits for each iris code, and compare them by using Hamming distance. Observing Table 1 and Table 2, that experimental results obtained on UBIRIS.v1 Sessao 1 shows that *cr-IR* is better than *ir-cr*, no matter what linear normalization algorithm or non-linear normalization algorithm are used. Besides, the results for CASIA.v1 normalized in *cr-IR* is better than in *ir-cr* with linear normalization algorithm. However, the results for CASIA.v1 with non-linear normalization are just in reverse, as listed in Table 1. Comparing eye images in two different databases, we found that the UBIRIS.v1 Sessao 1 has much complex furrows besides the collarette, and the texture under collarette is straight muscle. After unwrapping it, the divergence of texture of iris images in UBIRIS.v1 Sessao 1. presents lightly. Moreover, the iris furrows are complex near pupil in CASIA.v1, so the feature representation in *ir-cr* is better than in *ir-IR*.

Table I
EXPERIMENTAL RESULTS WITH LINE NORMALIZATION ALGORITHM (%)

	ir-IR	ir-cr	cr-IR
CASIA.v1	6.9	9.3	4.3
UBIRIS.v1 Sessao	3.5	4.5	3.7

Table II
EXPERIMENTAL RESULTS WITH NON-LINE NORMALIZATION ALGORITHM (%)

	ir-IR	ir-cr	cr-IR
CASIA.v1	3.5	4.3	9.6
UBIRIS.v1 Sessao 1	3.5	3.3	3.2

IV. CONCLUSION

In this paper, we propose a collarette detection method based on pixel intensity variation by using polynomial curve fitting, unlike existing variants of collarette by using a strong classifier. We only extract features with 2D-Gabor wavelet filter and store a small number of bits for each iris code, then compare them by using hamming distance, and set a threshold to classify them. Therefore, the experimental results show the effectiveness of our radius and collarette localization algorithms as well as iris normalization algorithm.

REFERENCES

[1] J. G. Daugman. High confidence visual recognition of persons by a test of statistical independence. *IEEE Transactions on Pattern Analysis and Machine Intelligence*, 15(11):1148–1161, 1993.

[2] R. P. Wildes. Iris recognition: An emerging biometric technology. *Proceedings of the IEEE*, 85(9):1348–1363, 1997.

[3] H. J. Wyatt. A 'minimum-wear-and-tear' meshwork for the iris. *Vision Research*, 40(16):2167–2176, 2000.

[4] X. Yuan and P. Shi. Iris recognition using collarette boundary localization. In *Proceedings of International Workshop on Biometric Recognition Systems on Advances in Biometric Person Authentication (IWBRS 2005)*, volume 4, pages 135–141, 2005.

[5] H Sung, J. Lim, J. H. Park, and Y. Lee. Iris recognition using collarette boundary localization. In *Proceedings of the 17th International Conference on Pattern Recognition (ICPR 2004)*, volume 4, pages 857–860, 2004.

[6] K. Roy and P. Bhattacharya. Collarette area localization and asymmetrical support vector machines for efficient iris recognition. In *Proceedings of the 14th International Conference on Image Analysis and Processing (ICIAP 2007)*, pages 3–8, 2007.

[7] Z. F He, T. N. Tan, Z. A. Sun, and X. C. Qiu. Toward accurate and fast iris segmentation for iris biometrics. *IEEE Transactions on Pattern Analysis and Machine Intelligence*, 31(9):1670–1684, 2009.

[8] C. M. Bishop. *Pattern Recognition and Machine Learning*. Springer, 1 edition, 2007.

[9] H. Proena and L. A. Alexandre. UBIRIS: A noisy iris image database. In *Proceedings of the 13th International Conference on Image Analysis and Processing (ICIAP 2005)*, volume LNCS 3617, pages 970–977, 2005.

[10] P. J Phillips, K. W Bowyer, and P. J Flynn. Comments on the CASIA version 1.0 iris data set. *IEEE Transactions on Pattern Analysis and Machine Intelligence*, 29(10):1869–1870, 2007.
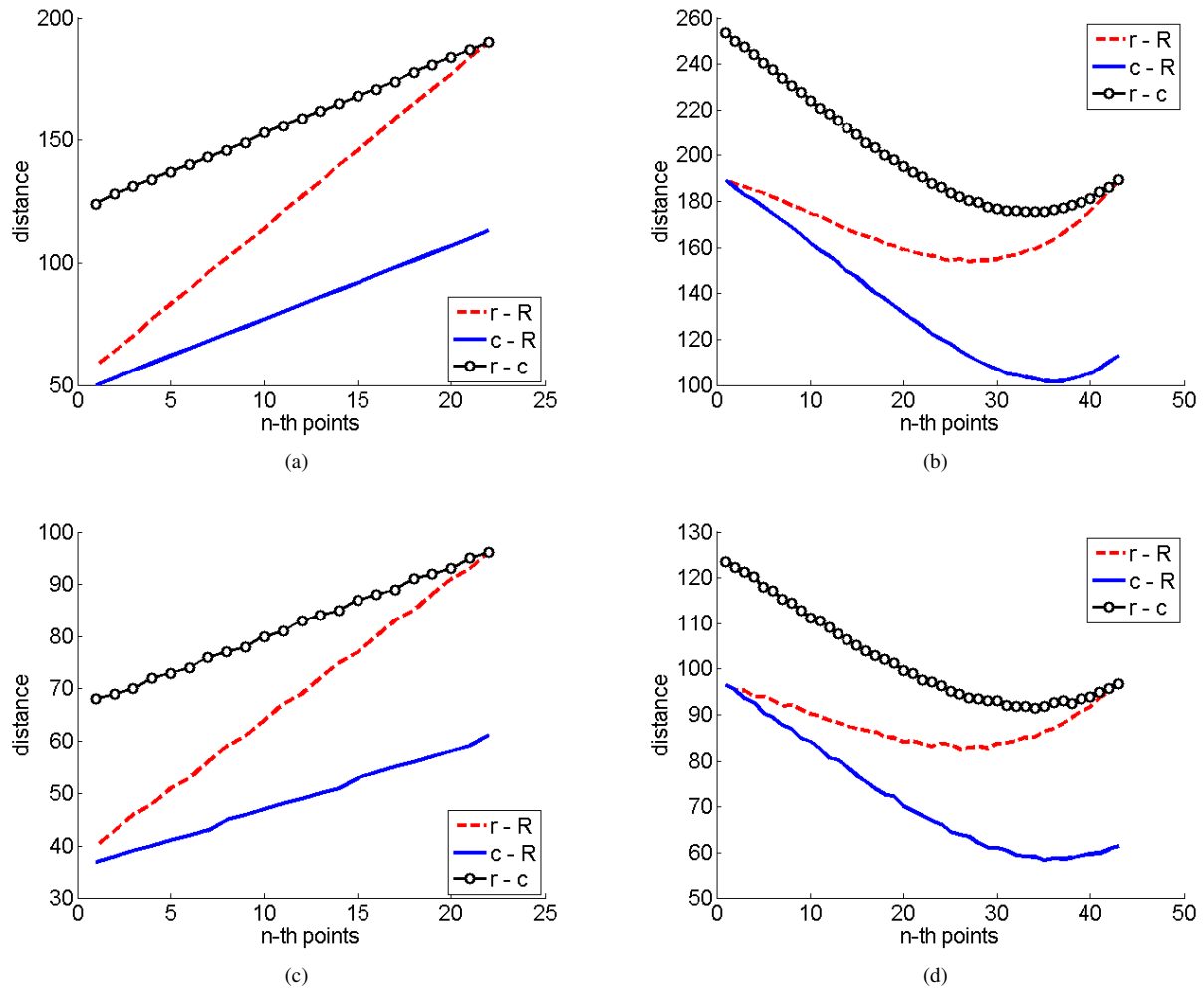
Figure 8.   The experimental performance in UBIRIS.v1 Sessao and CASIA.v1 with different iris localization methods and normalization algorithms. (a)(b) UBIRIS.v1 Sessao 1, (c)(d)CASIA.v1